Hybrid Nanostructures for Enhanced Light-Harvesting: Plasmon Induced Increase in Fluorescence from Individual Photosynthetic Pigment-Protein Complexes

ARTICLE *in* NANO LETTERS · NOVEMBER 2011

Impact Factor: 13.59 · DOI: 10.1021/nl202772h · Source: PubMed

6 AUTHORS, INCLUDING:

Stefan Kudera
Max Planck Institute for Intelligent Systems, …
48 PUBLICATIONS **3,949** CITATIONS
SEE PROFILE

Alastair Gardiner
University of Glasgow
84 PUBLICATIONS **1,876** CITATIONS
SEE PROFILE

Richard Cogdell
University of Glasgow
479 PUBLICATIONS **16,074** CITATIONS
SEE PROFILE

NANO LETTERS

LETTER

pubs.acs.org/NanoLett

Hybrid Nanostructures for Enhanced Light-Harvesting: Plasmon Induced Increase in Fluorescence from Individual Photosynthetic Pigment–Protein Complexes

Sebastian R. Beyer,[†] Simon Ullrich,[‡] Stefan Kudera,[‡] Alastair T. Gardiner,[§] Richard J. Cogdell,[§] and Jürgen Köhler*[,†]

[†]Experimental Physics IV and Bayreuther Institut für Makromolekülforschung (BIMF), University of Bayreuth, 95440 Bayreuth, Germany

[‡]Department of New Materials and Biosystems, Max-Planck-Institute for Intelligent Systems, 70569 Stuttgart, Germany

[§]College of Medical, Veterinary and Life Sciences, Institute of Molecular, Cell and Systems Biology, Biomedical Research Building, Glasgow G12 8QQ, Scotland, U.K.

Supporting Information

ABSTRACT: We studied the optical response from more than 13 000 individual photosynthetic pigment–protein complexes interacting with spherical gold nanoparticles. The nanodots were arranged in a quasi-hexagonal array by diblock copolymer micellar nanolithography. Exciting the proteins within the spectral range of the nanoparticles' plasmon resonance yields a clear enhancement of the protein fluorescence intensity, whereas excitation far out of the plasmon resonance features no effect. This result indicates a strategy for the construction of efficient hybrid light-harvesting devices.

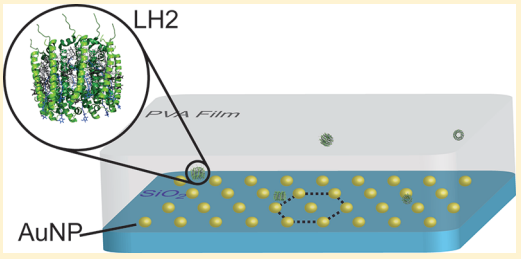

KEYWORDS: Plasmon enhancement, pigment–protein complexes, single molecule spectroscopy, LH2, hybrid nanostructures, *Rhodobacter sphaeroides*

Currently there is an enormous interest in trying to mimic photosynthetic systems to collect, direct, and use solar radiation.[1−4] Important issues that have to be considered when thinking of how to design such systems concern the character of the donor–acceptor materials, their chemical nature, their mutual arrangement (distance and orientation), their electronic couplings, their reorganization energies, and the influence of the surrounding matrix to optimize the energy- and charge-transfer properties of the supramolecular building blocks. Moreover the hierarchical organization of individual components must be precisely controlled so that devices can cover macroscopic surface areas without loss in efficiency. An alternative strategy is to take advantage of existing functional photosynthetic units, such as natural pigment–protein complexes, and use them as building blocks for the development of novel, biohybrid light-harvesting devices.[5−8] Arguments in favor of this strategy are that the protein matrix imposes a structural hierarchy that ensures the proper positioning of the cofactors and acts as a "smart matrix" forming a unique environment around the chromophores that promotes functionality. An important step forward to control the optical response of complex biomolecules has been reported by Mackowski et al.[9] who studied a peridinin-chlorophyll-protein (PCP), which is a photosynthetic antenna complex from algae. These authors showed that placing a PCP complex close to a silver island film resulted in an enhancement of the fluorescence intensity of these systems by more than 1 order of magnitude. This enhancement was attributed to a significant increase of the excitation rate of the antenna induced by excitations in the silver layer suggesting a novel route that can be used to improve the light-collection efficiency of the PCP complex. Recently, a similar enhancement of the absorption of photosystem I (PS I) from plants was observed in a study conducted on ensembles of PS I metal nanoparticle hybrids and on single PS I systems.[10] During the past decade it has been well established that the emission rate of a fluorescent dye can be significantly modified by coupling it resonantly to noble metal nanoparticles (NPs).[11−13] In such particles the conduction electrons can be excited collectively resulting in a plasmon. The details of the plasmon spectrum depend on the material, the dielectric constant of the surrounding medium, and the size/shape of the NP.[14−16] The extinction of light in resonance with the plasmon oscillation features not only an absorption component but also a strong scattering component, which produces new field components in the vicinity of the NP. As a consequence of this, the excitation and emission properties of a fluorophore close to the NP can be altered significantly. Both, quenching of the chromophores' fluorescence due to energy transfer to the NP and subsequent radiationless dissipation, as well as an increased emission due to the enhancement of the local electric field becomes possible.[17−19] The net effect of the change of the fluorescence rate of the

Received: August 10, 2011
Revised: September 29, 2011
Published: October 05, 2011

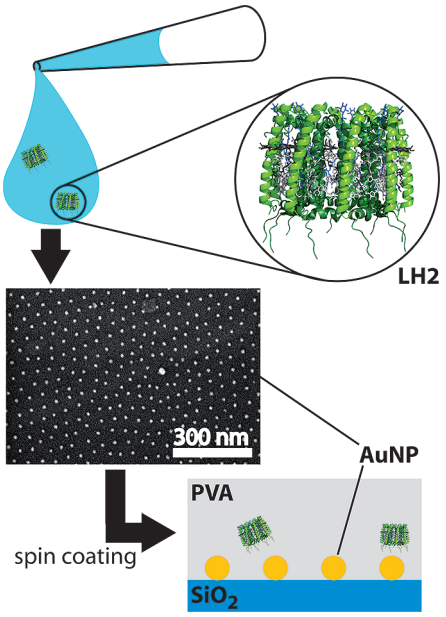

Figure 1. Top: A buffer solution containing 2% of PVA and a low concentration of LH2 complexes from *Rb. sphaeroides* was spin coated onto a fused silica (SiO_2) substrate. Center: Electron micrograph of the nanopatterned substrate that is covered with an array of gold nanoparticles (AuNP). Bottom: Schematic side view of the sample (not to scale) displaying the substrate (blue), AuNPs (yellow), LH2 (green), and the PVA matrix (gray). The thickness of the PVA layer is about 100 nm.

chromophore depends on the mutual arrangement of the chromophore and the noble metal NP, as well as the spectral overlap between the absorption spectrum of the chromophore and the plasmon resonance.[20,21] Meanwhile plasmon coupling of chromophores has been exploited for various biophysical applications for example for biomolecular recognition[22] or as a molecular ruler.[23,24] The work of Mackowski et al.[9] has demonstrated that the plasmon-induced amplification of the electromagnetic fields is also effective for chromophores that are embedded in a protein matrix.

However, any type of systematic tuning of the electronic properties of biological functional units requires a better control of the plasmon nanostructures. As a first step toward this goal we studied the optical response of individual light-harvesting 2 (LH2) complexes from photosynthetic purple bacteria that were deposited on a patterned surface covered with nanofabricated spherical gold nanoparticles (AuNPs). Fused silica (SiO_2) substrates were coated with AuNPs by diblock copolymer micelle nanolithography (BCML) following the procedure described in ref 25 (for materials and details on the method used in the preparation of AuNPs see Supporting Information). This resulted in a quasi hexagonal pattern of spherical AuNPs with a mean center-to-center distance of about 60 nm. The nanoparticles featured a narrow size distribution with an average diameter of (12.3 ± 1.3) nm. The plasmon resonance occurs at a peak position of 525 nm with a width of 260 nm (fwhm). The LH2 complexes from *Rhodobacter (Rb.) sphaeroides* (strain 241) were isolated and purified as described previously.[26] After purification the LH2 complexes were transferred into a buffer (20 mM TRIS/HCl, pH 8, 0.2% LDAO), aliquoted, and stored at −80 °C until used. For the present experiments this stock solution was diluted with buffer to 10^{-12} M and 2% polyvinyl alcohol (PVA) was added. Subsequently the material was spin coated onto an AuNP substrate forming an amorphous film with a thickness of about 100 nm that contained the LH2 complexes, see Figure 1. The low LH2 concentration ensures that the average distance between the LH2 complexes that interact with AuNPs is significantly larger than the resolving power of the optics employed. The LH2 complex from *Rb. sphaeroides* accommodates 27 BChl *a* molecules and 9 carotenoids. These proteins feature absorptions between 470−520 nm due to the carotenoids and around 800 and 850 nm due to the BChl *a* molecules. Owing to ultrafast energy transfer within these complexes their emission occurs predominantly from the B850 BChls at about 865 nm which corresponds to the lowest electronically excited state manifold.[27]

The samples were illuminated either at 514 nm (140 W/cm^2) by the output from an Ar-Ion laser (Innova 90, Coherent) or at 788 nm (140 W/cm^2) by a Titanium:Sapphire laser (Model 3900s, Spectra Physics) through a home-built microscope focusing the excitation light to a spot of 30 μm in diameter. The microscope objective (Euromex Holland, S.PlanM 60×, NA = 0.85) and the sample holder were accommodated in a recipient that was flushed with nitrogen gas to minimize photochemical reactions with oxygen. All experiments were performed at room temperature. The diameter of the excitation light was expanded and collimated with a telescope to about 20 mm from which the central 6 mm was cut out with an iris diaphragm. This ensured (within 5%) a uniform excitation intensity across the focal spot. The excitation was reflected toward the microscope via a dichroic mirror (530 DCXR, AHF analysentechnik AG), and the LH2 emission was collected by the same objective, long-pass filtered (LP545, LP635, LP808, AHF analysentechnik AG) and detected with an electron multiplying CCD camera (Andor iXon-EMCCD, Model X1214, exposure time 500 ms). For illumination at 788 nm the dichroic mirror was replaced by a 50/50 beam splitter and other long-pass filters (LP808, 2× LP830) were used. The CCD images were processed automatically, using home-written software, to identify the signals from individual complexes and to correct for background. This enabled us to evaluate the fluorescence response of more than 13 000 individual LH2 complexes.

The distributions of the fluorescence response from individual LH2 complexes are compared in Figure 2. For the top panel, Figure 2a, the samples were excited at 514 nm, that is, within the region of spectral overlap of LH2's absorption and the plasmon resonance of the AuNPs. Whereas for the lower panel, Figure 2b, the samples were excited at 788 nm, that is, far outside the overlap of the LH2's absorption and the plasmon resonance. The ensemble absorption spectrum of LH2 has equal extinction coefficients at these wavelengths, see insets Figure 2. This is why these particular wavelengths were chosen. However, since a direct comparison of the emission intensities at the two excitation wavelengths is hampered by several experimental factors, such as differences in the transmission characteristics and/or the collection efficiencies of the optical setup, or variations in focal size, at each excitation wavelength we conducted a control experiment on bare SiO_2 substrates without AuNPs, Figure 2 data shown in gray. From these controls, the mean fluorescence intensity, $\langle I_{ref} \rangle$, could be deduced for a LH2 complex in the absence of nanoparticles. In the following, the measured fluorescence intensities observed in the presence of the AuNPs will be given in units of the respective $\langle I_{ref} \rangle$ in order to allow direct comparisons.

Excitation of LH2 at 514 nm on bare SiO_2 substrates yields a distribution of the relative intensities with a mean value of 1.0 (by definition of $\langle I_{ref} \rangle$) and a standard deviation of 0.5. For the

dx.doi.org/10.1021/nl202772h |*Nano Lett.* 2011, 11, 4897–4901

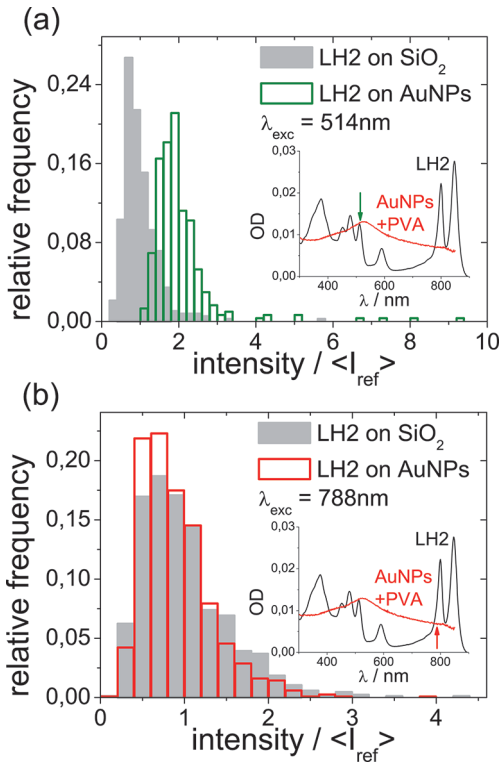

Figure 2. Distributions of the fluorescence response from individual LH2 complexes (a) for excitation at 514 nm and (b) for excitation at 788 nm. The insets display the absorption spectrum of LH2 (black line) overlaid with the plasmon resonance of the AuNPs in PVA (red line). The arrows indicate the wavelengths of 514 and 788 nm, respectively. The colored histograms have been obtained from LH2 complexes on substrates covered with AuNPs, and the gray histograms were recorded from LH2 complexes on bare SiO_2 substrates. For better comparison the histograms are scaled to relative occurencies, and the fluorescence intensities are given in units of $\langle I_{ref} \rangle$, which refers to the mean of the fluorescence intensity observed for the reference experiment on bare SiO_2 substrates (gray bars). The absolute number of LH2 complexes contributing to the histograms was (bare/covered substrate) 378/303 (panel a) and 867/1184 (panel b).

substrates covered with the gold spheres the respective histogram in Figure 2a is clearly shifted toward higher intensities and is characterized by a mean (standard deviation) of 2.0 (0.9). A few of the individual LH2 complexes had relative fluorescence intensities between 4.1 and 9.3 and one complex had a maximum intensity of 12.2. The histograms obtained from the experiment at 788 nm are displayed in Figure 2b and are characterized by a mean (standard deviation) of 1.0 (0.5) for the bare SiO_2 substrate and 0.9 (0.4) for the coated substrate, showing no significant statistical differences between these two distributions.

These data clearly reveal the influence of the plasmon resonance of the AuNPs on the fluorescence intensity of the pigment−protein complexes. The fact that we observe a broad range of enhancement factors can be ascribed to a distribution of distances and mutual orientations between the LH complexes and the NPs. In order to obtain a coarse grained estimate for the maximum distance between a LH2 and an AuNP for which the enhancement effect can be observed, we performed a similar experiment as described above yet with a slightly modified preparation of the sample. First the AuNP substrates were covered with an extra layer of PVA with a thickness of about (20 ± 5) nm and then the LH2-containing PVA solution was spin coated on top of this (for details on the characterization of the PVA film thickness see Supporting Information). This procedure ensured a minimum distance of about 20 nm between the LH2 complexes and the AuNPs. In this case, no enhancement of the LH2 emission due to the presence of the AuNPs could be observed (see Figure S2 Supporting Information) providing an upper limit of 20 nm for the maximum distance between the LH2 and the AuNPs for an observable enhancement effect.

An estimate for the enhanced absorption of a LH2 complex in the vicinity of a AuNP can be obtained by considering a metallic sphere that is illuminated by a plane wave $\vec{E}_{noNP} = \vec{E}_0 e^{-i\omega t} = E_0\, \hat{n}_{E_0} e^{-i\omega t}$. Here E_0 denotes the amplitude of the incident electric field, which is linearly polarized along the direction of the unit vector $\hat{n}_{E_0}$. In the limit where the size of the NP is much smaller than the wavelength of light, the dominating contribution to the scattered field comes from the dipolar component.[28] Within this approximation the electric potential in presence of the NP is given by[29]

$$\begin{aligned}\varphi_{NP} &= \varphi_{noNP} + \varphi_{scatter} \\ &= -\vec{E}_0 \cdot \vec{r} + R^3 \frac{\varepsilon_{NP} - \varepsilon_{medium}}{2\varepsilon_{medium} + \varepsilon_{NP}} \frac{\vec{E}_0 \cdot \vec{r}}{r^3} \end{aligned} \quad (1)$$

Here φ_{noNP} corresponds to the electric potential without NPs, ε_{NP} and ε_{Medium} denote the dielectric functions of the NP and the surrounding medium, respectively. R corresponds to the radius of the NP, and $\vec{r} = r\hat{n}_r$ refers to the radius vector from the origin, which is placed in the center of the NP. For brevity the time dependence of the electric field has been omitted. The amplitude of the electric field in the presence of the NP follows from $\vec{E}_{NP} = -\nabla\varphi_{NP}$ which yields

$$\vec{E}_{NP} = \vec{E}_0 - \beta\frac{R^3}{r^3}\vec{E}_0 + 3\beta\frac{R^3}{r^5}(\vec{E}_0 \cdot \vec{r})\,\vec{r} \quad (2)$$

using the abbreviation $\beta = (\varepsilon_{NP} - \varepsilon_{medium})/(2\varepsilon_{medium} + \varepsilon_{NP})$. The enhancement factor of the intensity of the electric field due to the presence of the NP can be defined as $P = |\vec{E}_{NP}|^2/|\vec{E}_{noNP}|^2$ which reads in this approximation

$$\begin{aligned} P &= 1 - 2\frac{R^3}{r^3}\mathrm{Re}(\beta)[1 - 3(\hat{n}_{E_0} \cdot \hat{n}_r)^2] \\ &\quad + \frac{R^6}{r^6}|\beta|^2[1 + 3(\hat{n}_{E_0} \cdot \hat{n}_r)^2] \end{aligned} \quad (3)$$

Averaging this expression over all directions finally yields

$$\langle P \rangle_r = 1 + 2\frac{R^6}{r^6}|\beta|^2 \quad (4)$$

which gives the enhancement factor of the intensity of the electric field as a function of the distance of the chromophore from the NP. Using eq 4 we calculated the distribution of the enhancement factors $\langle P \rangle_r$ within a spherical shell that surrounds the NP concentrically with an inner radius $R + \rho$ and a thickness d. For ε_{NP}, we used the dielectric function of gold as given in ref 30 and ε_{medium} was set to $\varepsilon_{PVA} = 2.19$. The distance ρ between the inner surface of the shell and the surface of the NP was set to 3 nm, which takes into account that the pigments are embedded in a protein matrix that is surrounded by a cage of surfactant molecules. However, when we try to relate the calculated

dx.doi.org/10.1021/nl202772h |Nano Lett. 2011, 11, 4897–4901

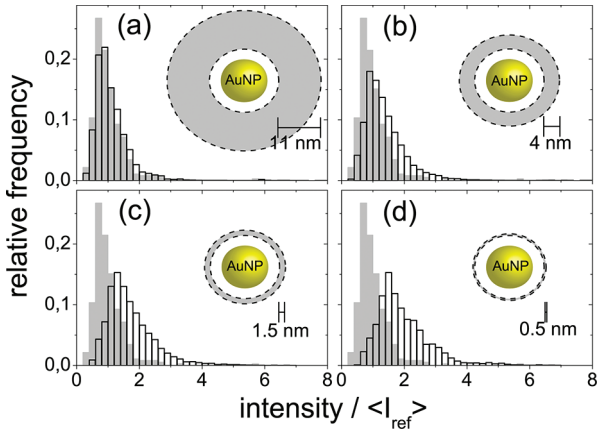

Figure 3. Calculated intensity distributions for the fluorescence enhancement of LH2 complexes (black) as a function of their distance from a single AuNP. The calculations were performed using a dipole approximation as explained in the text. The LH2 complexes were located within a shell of finite thickness d (gray area) that accommodates the AuNP (yellow) in its center. The distance between the surface of the AuNP and the inner surface of the shell was set to 3 nm, while the thickness d of the shell was varied from 11 nm (top left) to 0.5 nm (bottom right). The intensities are given in units of $\langle I_{ref} \rangle$, which corresponds to the mean of the intensity distribution obtained experimentally from LH2 on bare SiO_2 (gray). The mean (standard deviation) of the simulated histograms are (a) 1.1 (0.6), (b) 1.4 (0.7), (c) 1.7 (0.9), and (d) 2.0 (1.0).

distribution of the enhancement factors to the experimentally observed intensity distribution of the LH2 fluorescence, we face the problem that the fluorescence intensity from individual LH2 complexes already features a distribution without any NPs, see Figure 2a (gray bars). Therefore we convoluted the simulated distribution for the enhancement factors with the distribution of the fluorescence intensity of the LH2 complexes that is observed on bare SiO_2 substrates NPs. The result of this procedure is shown in Figure 3 for d varying from 0.5 to 11 nm, together with the measured reference distributions of the fluorescence intensity in the absence of NPs (light gray). An enhancement of the LH2 fluorescence that resembles the experimentally obtained intensity distribution is found only if the distance between the AuNP and the pigments falls into the range of 3−5 nm. This finding is consistent with the result from the control experiment with the extra PVA layer. The conjecture that the LH2 complexes seem to stick to the AuNPs within a thin layer of only a few nanometers thickness is in line with the well-known fact that proteins tend to adsorb on noble metal surfaces.[31]

The result of this study opens the possibility to use noble metal nanoparticles for tuning the photophysical properties of integral membrane antenna complexes in a well-defined way and to optimize the architecture of biohybrid light-harvesting structures.

■ ASSOCIATED CONTENT

Supporting Information. Materials and method for AuNP preparation, characterization of PVA-film thickness, and reference experiment with spacer. This material is available free of charge via the Internet at http://pubs.acs.org.

■ AUTHOR INFORMATION

Corresponding Author
*E-mail: juergen.koehler@uni-bayreuth.de.

■ ACKNOWLEDGMENT

We thank J. Spatz for fruitful discussions. Financial support from the German Science Foundation (Ko 1359/21-1; GRK 1640) is gratefully acknowledged. R.J.C. and A.T.G. thank the EPSRC for financial support.

■ REFERENCES

(1) Nagata, N.; Kuramochi, Y.; Kobuke, Y. *J. Am. Chem. Soc.* **2009**, *131*, 10–11.
(2) Uemura, S.; Sengupta, S.; Würthner, F. *Angew. Chem.* **2009**, *121*, 7965–7968.
(3) Sengupta, S.; Uemura, S.; Patwardhan, S.; Huber, V.; Grozema, F. C.; Siebbeles, L. D. A.; Baumeister, U.; Würthner, F. *Chem.—Eur. J.* **2011**, *17*, 5300–5310.
(4) Balaban, T. S. *Acc. Chem. Res.* **2005**, *38*, 612–623.
(5) Lebedev, N.; Trammell, S. A.; Tsoi, S.; Spano, A.; Kim, J. H.; Xu, J.; Twigg, M. E.; Schnur, J. M. *Langmuir* **2008**, *24*, 8871–8876.
(6) Oda, I.; Iwaki, M.; Fujita, D.; Tsutsui, Y.; Ishizaka, S.; Dewa, M.; Nango, M.; Kajino, T.; Fukushima, Y.; Itoh, S. *Langmuir* **2010**, *26*, 13399–13406.
(7) Escalante, M.; Zhao, Y.; Ludden, M. J. W.; Vermeij, R.; Olsen, J. D.; Berenschot, E.; Hunter, C. N.; Huskens, J.; Subramaniam, V.; Otto, C. *J. Am. Chem. Soc.* **2008**, *130*, 8892–8893.
(8) Grimme, R. A.; Lubner, C. E.; Bryant, D. A.; Golbeck, J. H. *J. Am. Chem. Soc.* **2008**, *130*, 6308–6309.
(9) Mackowski, S.; Wörmke, S.; Maier, A. J.; Brotosudarmo, T. H. P.; Harutyunyan, H.; Hartschuh, A.; Govorov, A. O.; Scheer, H.; Bräuchle, C. *Nano Lett.* **2008**, *8*, 558–564.
(10) (a) Carmeli, I.; Lieberman, I.; Kraversky, L.; Fan, Z.; Govorov, A. O.; Markovich, G.; Richter, S. *Nano Lett.* **2010**, *10*, 2069–2074. (b) Nieder, J. B.; Bittl, R.; Brecht, M. *Angew. Chem. Int. Ed.* **2010**, *49*, 10217–10220.
(11) Dulkeith, E.; Ringler, M.; Klar, T. A.; Feldmann, J.; Muñoz Javier, A.; Parak, W. J. *Nano Lett.* **2005**, *5*, 585–589.
(12) Muskens, O. L.; Giannini, V.; Sánchez-Gil, J. A.; Gómez Rivas, J. *Nano Lett.* **2007**, *7*, 2871–2875.
(13) Bharadwaj, P.; Beams, R.; Novotny, L. *Chem. Sci.* **2011**, *2*, 136–140.
(14) Sönnichsen, C.; Franzl, T.; Wilk, T.; von Plessen, G.; Feldmann, J. *New J. Phys.* **2002**, *4*, 93.1–93.8.
(15) Schubert, O.; Becker, J.; Carbone, L.; Khalavka, Y.; Provalska, T.; Zins, I.; Sönnichsen, C. *Nano Lett.* **2008**, *8*, 2345–2350.
(16) Sönnichsen, C.; Franzl, T.; Wilk, T.; von Plessen, G.; Feldmann, J. *Phys. Rev. Lett.* **2002**, *88*, 077402.
(17) Anger, P.; Bharadwaj, P.; Novotny, L. *Phys. Rev. Lett.* **2006**, *96*, 113002.
(18) Bharadwaj, P.; Anger, P.; Novotny, L. *Nanotechnology* **2007**, *18*, 044017.
(19) Chen, Y.; Munechika, K.; Jen-La Plante, I.; Munro, A. M.; Skrabalak, S. E.; Xia, Y.; Ginger, D. S. *Appl. Phys. Lett.* **2008**, *93*, 053106.
(20) Bek, A.; Jansen, R.; Ringler, M.; Mayilo, S.; Klar, T. A.; Feldmann, J. *Nano Lett.* **2008**, *8*, 485–490.
(21) Chen, Y.; Munechika, K.; Ginger, D. S. *Nano Lett.* **2007**, *7*, 690–696.
(22) Baciu, C. L.; Becker, J.; Janshoff, A.; Sönnichsen, C. *Nano Lett.* **2008**, *8*, 1724–1728.
(23) Sönnichsen, C.; Reinhard, B.; M. Liphardt, J.; Alivisatos, A. P. *Nat. Biotechnol.* **2005**, *23*, 741–745.
(24) Liu, N.; Hentschel, M.; Weiss, T.; Alivisatos, A. P.; Giessen, H. *Science* **2011**, *332*, 1407–1410.

(25) Glass, R.; Müller, M.; Spatz, J. P. *Nanotechnology* **2003**, *14*, 1153–1160.
(26) Gardiner, A. T.; Cogdell, R. J.; Takaichi, S. *Photosynth. Res.* **1993**, *38*, 159–167.
(27) Cogdell, R. J.; Gall, A.; Köhler, J. *Q. Rev. Biophys.* **2006**, *39*, 227–324.
(28) van Dijk, M. A.; Tchebotareva, A. L.; Orrit, M.; Lippitz, M.; Berciaud, S.; Lasne, D.; Cognet, L.; Lounis, B. *Phys. Chem. Chem. Phys.* **2006**, *8*, 3486–3495.
(29) Govorov, A. O.; Carmeli, I. *Nano Lett.* **2007**, *7*, 620–625.
(30) Johnson, P. B.; Christy, R. W. *Phys. Rev. B* **1972**, *6*, 4370–4379.
(31) Adams, J.; Tizazu, G.; Janusz, S.; Brueck, S. R. J.; Lopez, G. P.; Leggett, G. J. *Langmuir* **2010**, *26*, 13600–13606.

NOTE ADDED AFTER ASAP PUBLICATION

This article was published ASAP on October 10, 2011. Reference 10(b) has been added. The corrected version was posted on October 26, 2011.